

# Densification and grain growth of SiO<sub>2</sub>-doped ZnO

Nuray Canikoğlu, Nil Toplan, Kenan Yıldız, H. Özkan Toplan\*

*Department of Metallurgy and Materials Engineering, Sakarya University, Sakarya, Turkey*

Received 11 November 2004; received in revised form 22 November 2004; accepted 15 January 2005

Available online 21 March 2005

## Abstract

The grain growth kinetics in the 1, 2, 3 and 4 wt.% SiO<sub>2</sub> doped ZnO was studied using the simplified phenomenological grain growth kinetics equation  $G^n - G_0^n = K_0 \exp(-Q/RT)$  together with microstructure properties and densification of the sintered samples. The grain growth exponent values ( $n$ ) were found to be 3 for 1 wt.% SiO<sub>2</sub> doped ZnO, 6 for 2 and 3 wt.% SiO<sub>2</sub> doped ZnO and 7 for 4 wt.% SiO<sub>2</sub> doped ZnO. The apparent activation energy of 486 kJ/mol was found for 1 wt.% SiO<sub>2</sub> added system. A sharp increase in the apparent activation energy to a value of 900, 840 and 935 kJ/mol was found for 2, 3 and 4 wt.% SiO<sub>2</sub> added system, respectively. The apparent activation energy was increased with doping of SiO<sub>2</sub> because of the formation of spinel Zn<sub>2</sub>SiO<sub>4</sub> phase at the grain boundaries. This spinel phase inhibited the grain growth of ZnO. Also densification decreased with increasing SiO<sub>2</sub> doping.

© 2005 Elsevier Ltd and Techna Group S.r.l. All rights reserved.

**Keywords:** D. ZnO; E. Varistor; SiO<sub>2</sub> doping; Grain growth kinetics; Densification

## 1. Introduction

ZnO-based materials have been developed for various technological applications, such as varistors, gas sensors, and optoelectronic devices, due to their electrical and optical properties [1]. A typical ZnO based varistor is a very complex chemical system and contains several dopants, such as Bi, Sb, Mn, Cr, Co, Ti and Al [2].

The electrical properties of ZnO varistors directly depend on the composition and microstructural characteristics, such as grain size, density, morphology and the distribution of second phases. Many studies have been conducted on the sintering of several doped ZnO systems, such as Bi<sub>2</sub>O<sub>3</sub>-doped ZnO [3,4], Sb<sub>2</sub>O<sub>3</sub>-doped ZnO [5], Al<sub>2</sub>O<sub>3</sub>-doped ZnO [1], PbO-doped ZnO [6], CuO-doped ZnO [7]. Among the numerous works published on the subject, Senda and Bradt

[3] presented the most detailed study covering the grain growth kinetics in ZnO ceramics containing up to 4 wt.% Bi<sub>2</sub>O<sub>3</sub>. In their work, Senda and Bradt [3] used simplified grain growth kinetics equation

$$G^n = kt \exp\left(-\frac{Q}{RT}\right) \quad (1)$$

where  $G$  is the average grain size at time  $t$ ,  $n$  is the kinetic grain growth exponent value,  $k$  is a constant,  $Q$  is the apparent activation energy,  $R$  is the gas constant and  $T$  is the absolute temperature. Using this equation, Senda and Bradt have calculated the grain growth exponent value ( $n$ ) as 3 and apparent activation energy ( $Q$ ) as  $224 \pm 16$  kJ/mol in the sintering of the pure ZnO system.

The additions of MnO [8] and CoO [9] to the ZnO–6 wt.% Bi<sub>2</sub>O<sub>3</sub> system, the addition of MnO [10] to the ZnO–6 wt.% Sb<sub>2</sub>O<sub>3</sub> system and the addition of PbO [6] and CuO [7] to ZnO were studied by our group and the present work is the continuation of the previous works in the grain growth kinetics of ZnO varistors. The aim of the present work is also to study the effect of SiO<sub>2</sub> addition on microstructure and the sintering behaviour of ZnO.

\* Corresponding author. Tel.: +90 264 3460154; fax: +90 264 3460155.  
E-mail address: toplan@sakarya.edu.tr (H.Ö. Toplan).

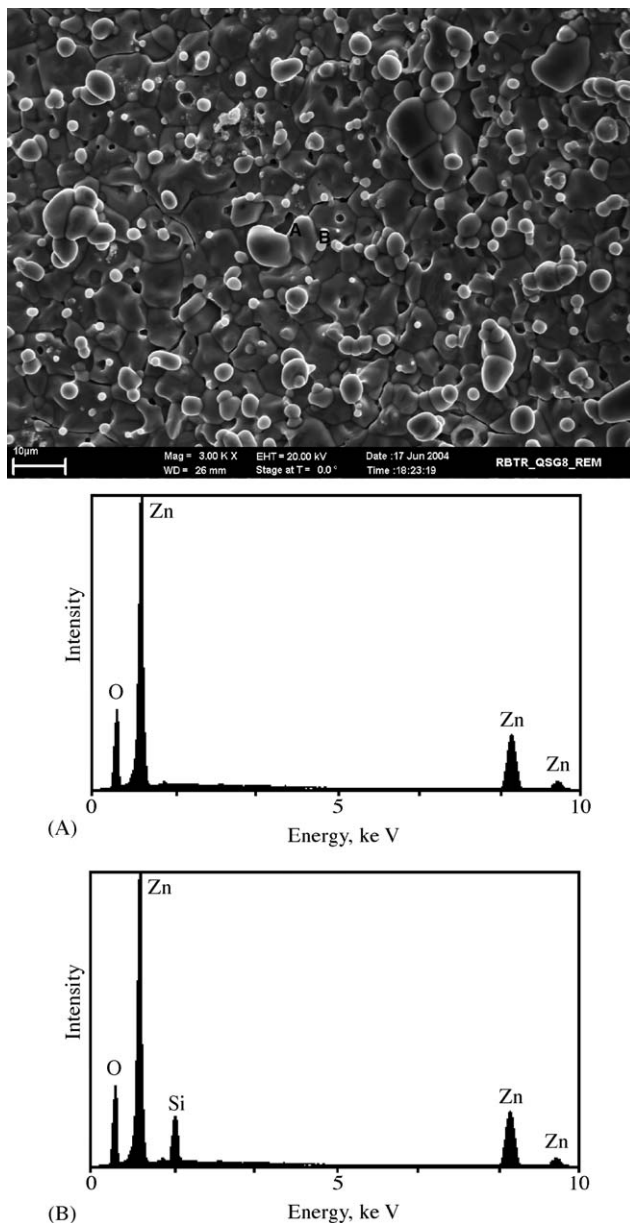


Fig. 1. The backscattered electron images and EDS of the 3 wt.% SiO<sub>2</sub>-doping ZnO sample sintered at 1300 °C for 5 h.

## 2. Experimental

High purity ZnO (99.7% Metal Bileşikleri A.Ş., Gebze, Turkey) and SiO<sub>2</sub> powders (pure grade) were used in preparation of four basic compositions; ZnO containing 1, 2, 3 and 4 wt.% SiO<sub>2</sub>. ZnO powders revealed a needle like fine crystal ca. 0.5 µm in width and ca. 0.5–2 µm in length. The calculated amounts of oxides for the indicated compositions were ball milled in ashless rubber lined ceramic jars for 6 h using zirconia balls and distilled water as the milling media. The mixtures were dried to ca. 10–15% moisture level and then granulated. Samples of 10 mm in diameter and ca. 8 mm in thick were prepared by semi-dry pressing of the granules of –150 µm + 75 µm in size range at a pressure of

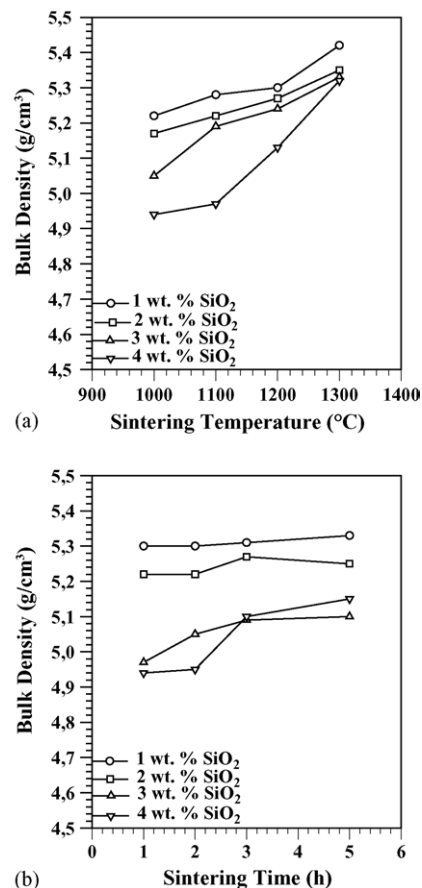


Fig. 2. The bulk density vs. sintering temperature (a) and the bulk density vs. sintering time (b) for SiO<sub>2</sub> doped ZnO.

100 MPa. The specimens were sintered at 1000, 1100, 1200 and 1300 °C for 1, 2, 3 and 5 h using a heating rate of 5 °C/min and were naturally cooled in a PID controlled furnace.

The bulk densities of the samples were calculated from their weight and dimensions. Characterizations of the phases in the sintered specimens were carried out by X-ray diffraction using Cu Kα radiation. For the microstructural observations, both scanning electron microscopy (SEM) of the fracture surfaces and optical microscopy of polished and etched surfaces were used. Grain size measurements were carried out on the micrographs of the etched samples using the following equation:

$$G = 1.56\bar{L} \quad (2)$$

where  $G$  is the average grain size,  $\bar{L}$  is the average grain boundary intercept length of four random lines on two different micrographs of each sample [11].

## 3. Results and discussion

### 3.1. Physical properties of the sintered samples

It was determined the presence of ZnO (ASTM Card No.: 5-0664) and Zn<sub>2</sub>SiO<sub>4</sub> (ASTM Card No.: 14-653)



phases by using of the X-ray powder diffraction of the  $\text{SiO}_2$ -added samples sintered at different temperatures for different periods of time.  $\text{SiO}_2$  formed a spinel phase ( $\text{Zn}_2\text{SiO}_4$ ) with ZnO as expected from the phase diagram of

the ZnO– $\text{SiO}_2$  binary system [12]. The backscattered electron images and energy dispersive X-ray spectrometer (EDS) of the 3 wt.%  $\text{SiO}_2$ -added ZnO samples sintered at 1300 °C for 5 h are given in Fig. 1. The micrograph clearly

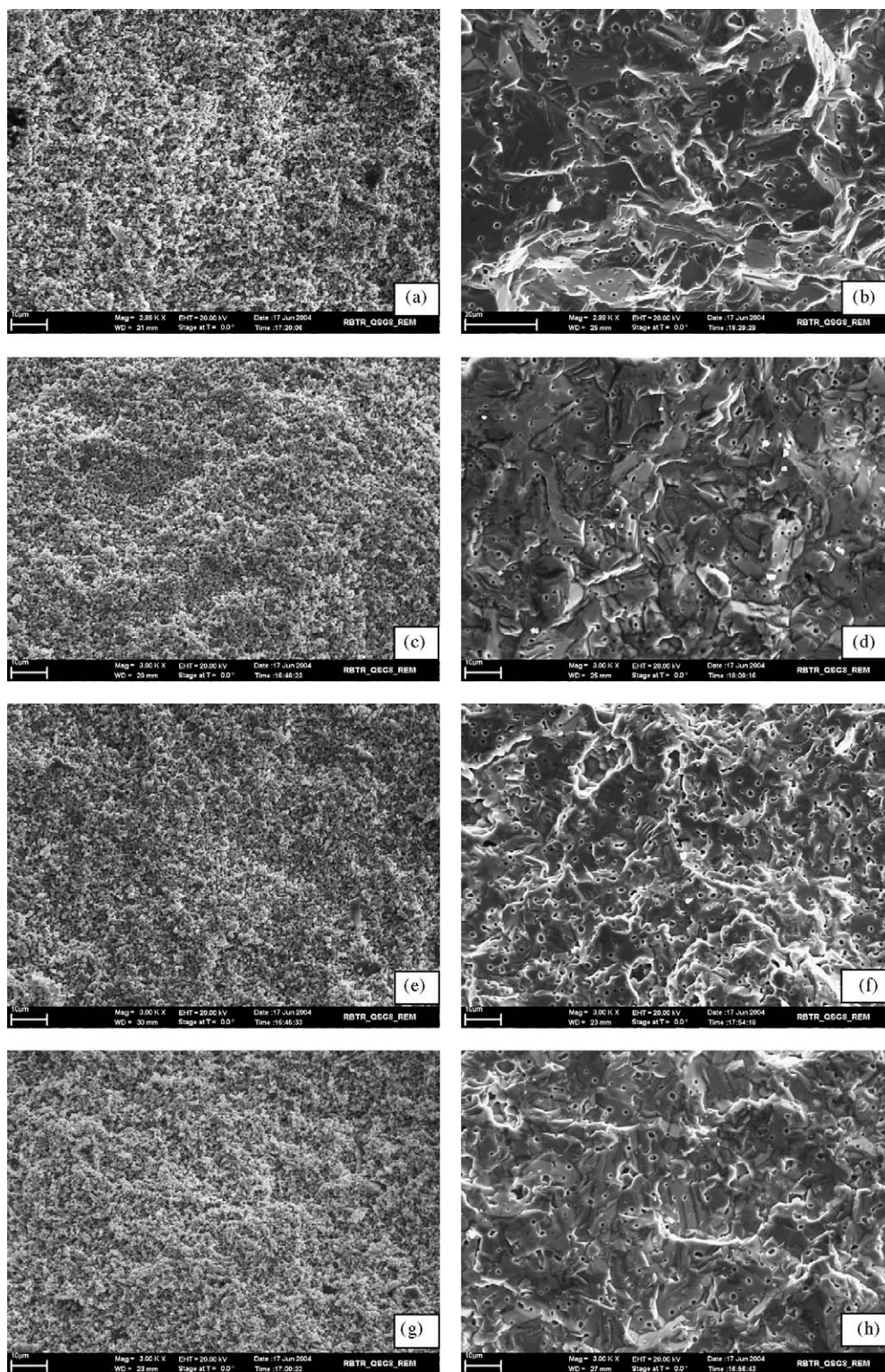


Fig. 3. SEM micrographs of the fracture surfaces of the samples with 1, 2, 3 and 4 wt.%  $\text{SiO}_2$  doping sintered at 1000 °C/1 h (a, c, e and g) and 1300 °C/1 h (b, d, f and h).

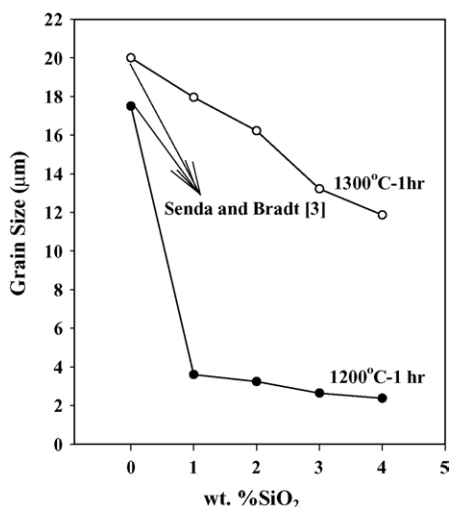


Fig. 4. The relationship between the average grain size and the level of SiO<sub>2</sub>-doping for the samples sintered at 1200 and 1300 °C for 1 h.

shows the spinel phases (Zn<sub>2</sub>SiO<sub>4</sub>) as bright regions between the ZnO grains.

The effects of sintering temperatures (°C) and sintering time (h) on the bulk densities of the specimens with different SiO<sub>2</sub> contents are given in Fig. 2(a and b). The highest densifications are obtained at high sintering temperatures and high sintering times. The bulk densities of SiO<sub>2</sub>-doped ZnO samples decreased markedly with increasing in the SiO<sub>2</sub> doping level. This reduction mainly arises from the differences between the densities of ZnO (5.68 g/cm<sup>3</sup>) and SiO<sub>2</sub> (2.63 g/cm<sup>3</sup>).

### 3.2. Grain growth kinetics

The SEM micrographs of the fracture surfaces of the samples with 1, 2, 3 and 4 wt.% SiO<sub>2</sub> content sintered at 1000 and 1300 °C for 1 h were compared in Fig. 3(a)–(f). The samples sintered at 1000 °C for 1 h resulted in a porous and fine (<1 μm) crystalline microstructure. The

sinterings at 1300 °C cause a sudden grain growth, which in turn entraps porosity within and among grains. Also the average grain size of each sample increases with increasing sintering temperature from 1000 to 1300 °C. As seen in Fig. 3, the grain growth of ZnO is inhibited because of the formation of Zn<sub>2</sub>SiO<sub>4</sub> phase in the grain boundaries with increasing of SiO<sub>2</sub>-doping level. The relationship between the average grain size and the level of SiO<sub>2</sub>-doping for the samples sintered at 1200 and 1300 °C for 1 h is given in Fig. 4. As seen from this figure, the average grain size of undoped ZnO is about 17.5 μm at 1200 °C for 1 h sintering and about 20 μm at 1300 °C for 1 h [3]. The average grain size of ZnO decreases with the SiO<sub>2</sub> additions. A sharp decrease in the grain size of the samples sintered at 1200 °C for 1 h is observed. The grain growth of ZnO is occurred with the solid-state diffusion of Zn<sup>+2</sup> cations. The solid-state diffusion of Zn<sup>+2</sup> cations is strongly inhibited by the formation of Zn<sub>2</sub>SiO<sub>4</sub> phase in the grain boundaries at the sintering of 1200 °C. (The grain size of ZnO is 3.6 μm in the 1 wt.% SiO<sub>2</sub>-doping.) But the same situation is not observed at the sintering of 1300 °C because of positive effect of this temperature on the solid-state diffusion. (The grain size of ZnO is 17.6 μm in the 1 wt.% SiO<sub>2</sub>-doping.)

The grain growth kinetics can be determined using the simplified phenomenological kinetics (Eq. (1)). The grain growth exponent value (*n*) in the equation can be found at isothermal conditions where the kinetic equation is expressed in the form of

$$n \log G = \log t + \left[ \log K_0 - 0.434 \left( \frac{Q}{RT} \right) \right] \quad (5)$$

The *n* value can be calculated from the slope of the log (grain size) versus log(time) line plot which is equal to (1/*n*). Such plots were made for isothermal conditions employed at the sintering temperatures and the (*n*) values were calculated from the slopes of the plots constructed by the linear regression method. Fig. 5(a)–(b) depicts the log *G* versus log *t* plots for different SiO<sub>2</sub> contents at the 1200 and

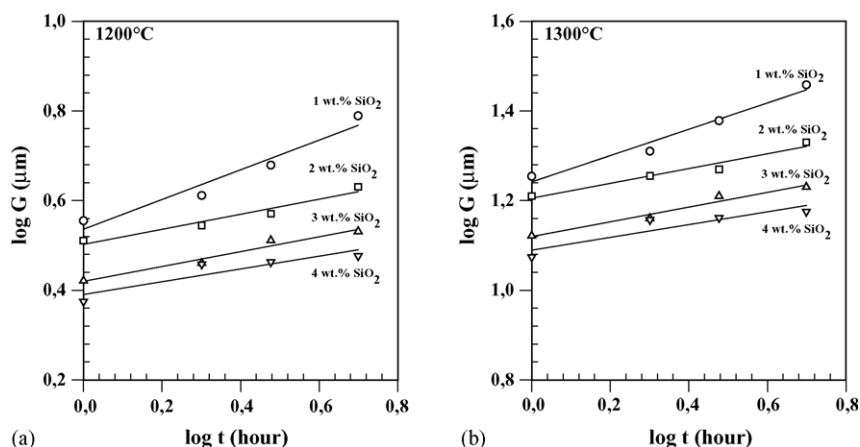


Fig. 5. Isothermal grain growth of ZnO with doping 1–4 wt.% SiO<sub>2</sub> sintered at (a) 1200 °C and (b) 1300 °C.

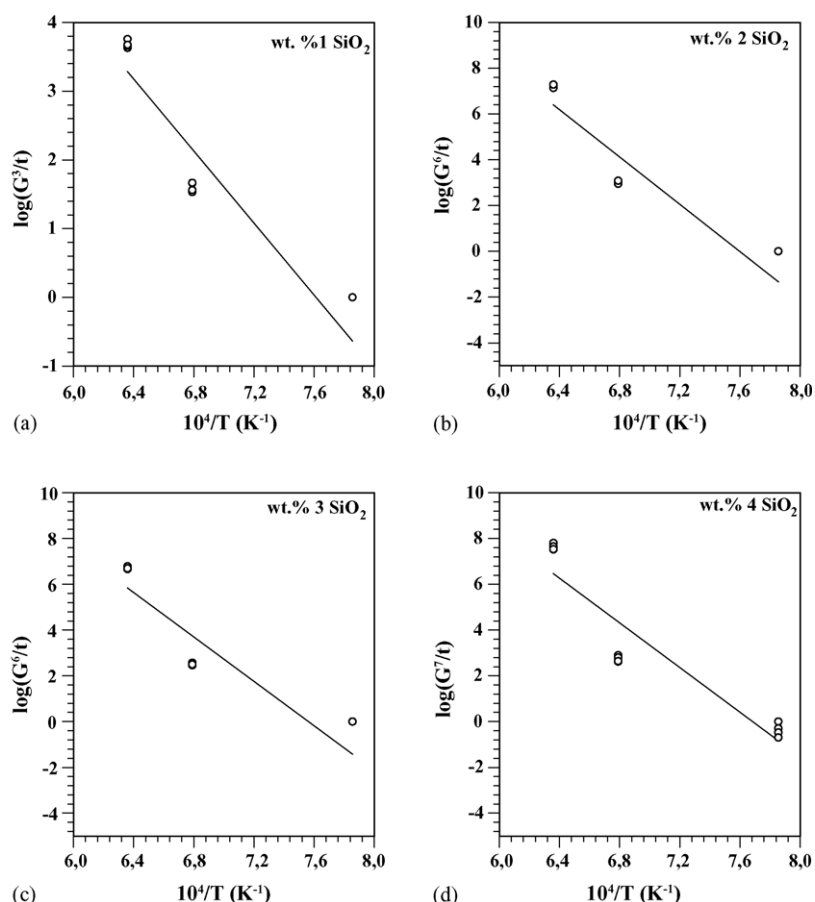


Fig. 6. Arrhenius plots for the grain growth of ZnO with doping 1–4 wt.% SiO<sub>2</sub> (a–d).

1300 °C temperatures and the calculated ( $n$ ) values are listed in Table 1. Similar plots could not be constructed for isothermal sintering at 1000 and 1100 °C, since the samples had a fine crystalline size (<1 µm) and a very porous microstructure, which gave rise to a large amount of grain pull-outs in the sample polishing process for optical microscopy. Therefore, the grain size values used as a starting point for plots in the evaluation of the activation energies were deduced from the SEM micrographs in the samples sintered only at 1000 °C.

Bradt and coworkers [3–5] have reported the  $n$  values for ZnO and ZnO–2.38 wt.% Sb<sub>2</sub>O<sub>3</sub> system as 3 and 6, respectively. They also pointed out that  $n$  value in a system indicated a grain growth inhibition mechanism. The  $n$  values for grain growth of the ZnO–1, 2, 3 and 4 wt.% SiO<sub>2</sub> system

studied in this work were found to be 3, 6, 6 and 7, respectively. It was found that the  $n$  value was affected by the high level of SiO<sub>2</sub> addition.

If Eq. (2) is expressed in the form of

$$\log\left(\frac{G^n}{t}\right) = \left[\log K_0 - 0.434\left(\frac{Q}{RT}\right)\right] \quad (6)$$

the apparent activation energy  $Q$  of a grain growth process can be calculated from the gradient of the Arrhenius plot of  $\log(G^n/t)$  versus  $1/T$  (K<sup>-1</sup>). Such plots for the studied system are given in Fig. 6(a–d). Table 1 also listed the  $n$  values accepted in the construction of these plots along with the calculated values of the logarithm of rate constants and the apparent activation energy. The numerous studies on the grain growth kinetics of ZnO have revealed that the rate controlling mechanism is the solid-state diffusion of Zn<sup>+2</sup> cations. The apparent activation energy for this process is about 225 kJ/mol. As indicated in Table 1, the apparent activation energy of 486 kJ/mol was found for 1 wt.% SiO<sub>2</sub> added system. A sharp increase in the apparent activation energy to a value of 900, 840 and 935 kJ/mol was found for 2, 3 and 4 wt.% SiO<sub>2</sub> added system, respectively.

Since the microstructural and phase analysis of SiO<sub>2</sub> containing ZnO ceramics indicates the presence of the Zn<sub>2</sub>SiO<sub>4</sub> spinel as distinct crystals at the grain boundaries,

Table 1

Calculated grain growth exponent ( $n$ ), apparent activation energy ( $Q$ ) and preexponential constant ( $K_0$ ) values

SiO <sub>2</sub> content (wt.%)	$n$ values used in Arrhenius plots	$\log K_0$	$Q$ (kJ/mol)
1	3	19.46	486
2	6	36.33	900
3	6	33.47	840
4	7	37.54	935



inhibition of the ZnO grain growth must be considered to be related to presence of those spinel grains. The type of grain growth inhibition has been previously reported for other ZnO systems such as ZnO–Sb<sub>2</sub>O<sub>3</sub> (Zn<sub>7</sub>Sb<sub>2</sub>O<sub>12</sub>) [5], ZnO–Al<sub>2</sub>O<sub>3</sub> (ZnAl<sub>2</sub>O<sub>4</sub>) [1], ZnO–TiO<sub>2</sub> (Zn<sub>2</sub>TiO<sub>4</sub>) [13].

#### 4. Conclusions

The effects of SiO<sub>2</sub> additions on the grain growth of ZnO were studied. SiO<sub>2</sub> additions at levels from 1 to 4 wt.% were investigated for sintering in air at temperatures from 1000 to 1300 °C and for 1–5 h. The resulting microstructures were observed by optical and electron microscopy and the phases were identified by the X-ray diffraction.

The apparent activation energy of 486 kJ/mol was found for 1 wt.% SiO<sub>2</sub> added system. A sharp increase in the apparent activation energy to a value of 900, 840 and 935 kJ/mol was found for 2, 3 and 4 wt.% SiO<sub>2</sub> added system, respectively. The apparent activation energy was increased with doping of SiO<sub>2</sub>. The addition of SiO<sub>2</sub> to ZnO inhibits strongly the grain growth of ZnO. The inhibition is dependent on SiO<sub>2</sub> content, so increased levels of SiO<sub>2</sub> yield finer average ZnO grain size. When SiO<sub>2</sub> is added to ZnO, Zn<sub>2</sub>SiO<sub>4</sub> spinel particles form at the grain boundaries. It appears to be dominated by a grain boundary particle drag mechanism that is related to the formation of second-phase Zn<sub>2</sub>SiO<sub>4</sub> spinel particles. The SiO<sub>2</sub> additions reduce the densification in the initial stages of sintering.

#### References

- [1] J. Han, P.Q. Mantas, A.M.R. Senos, Densification and grain growth of Al-doped ZnO, *J. Mater. Res.* 16 (2) (2001) 459–468.
- [2] J. Han, P.Q. Mantas, A.M.R. Senos, Grain growth in Mn-doped ZnO, *J. Eur. Ceram. Soc.* 20 (2000) 2753–2758.
- [3] T. Senda, R.C. Bradt, Grain growth in sintering ZnO and ZnO–Bi<sub>2</sub>O<sub>3</sub> ceramics, *J. Am. Ceram. Soc.* 73 (1) (1990) 106–114.
- [4] D. Dey, R.C. Bradt, Grain growth in sintering ZnO and ZnO–Bi<sub>2</sub>O<sub>3</sub> ceramics, *J. Am. Ceram. Soc.* 75 (9) (1992) 2529–2534.
- [5] T. Senda, R.C. Bradt, Grain growth of zinc oxide during the sintering of zinc oxide-antimony oxide ceramics, *J. Am. Ceram. Soc.* 74 (6) (1991) 1296–1302.
- [6] H.Ö. Toplan, H. Erkalfa, O.T. Özkan, The effect of the PbO addition on the sintering of ZnO, *Ceramics-Silikaty* 47 (3) (2003) 116–119.
- [7] F. Apaydin, H.Ö. Toplan, K. Yildiz, Effect of CuO on the grain growth of ZnO, *J. Mater. Sci.*, in press.
- [8] O.T. Özkan, M. Avcı, E. Oktay, H. Erkalfa, Grain growth in MnO-added ZnO 6 wt.% Bi<sub>2</sub>O<sub>3</sub> ceramic system, *Ceram. Int.* 24 (1988) 151–156.
- [9] V. Günay, O. Gelecek-Sulan, O.T. Özkan, Grain growth kinetic in  $x\text{CoO}-(6-x)\text{wt.}\% \text{Bi}_2\text{O}_3-(94-x)\text{ZnO}$  ( $x=0, 2, 4$ ) ceramic system, *Ceram. Int.* 30 (2004) 105–110.
- [10] Ö. Toplan, V. Günay, O.T. Özkan, Grain growth in the MnO added ZnO–6 wt.% Sb<sub>2</sub>O<sub>3</sub> ceramic system, *Ceram. Int.* 23 (1997) 251–255.
- [11] Metals Handbooks, vol. 8, eighth ed., American Society for Metals, Warrendale, PA, USA, 1973, p. 46.
- [12] E.M. Levin, C. Robbins, F. McMurdie, Phase Diagrams for Ceramics, The American Ceramic Society Inc., Columbus, OH, 1965, p. 120.
- [13] H.Ö. Toplan, Y. Karakaş, Grain growth in TiO<sub>2</sub>-added ZnO–Bi<sub>2</sub>O<sub>3</sub>–CoO–MnO ceramics prepared by chemical processing, *Ceram. Int.* 28 (2002) 911–915.